applied sciences

MDPI

Article

Hot Rolling of ZK60 Magnesium Alloy with Isotropic Tensile Properties from Tubing Made by Shear Assisted Processing and Extrusion (ShAPE)

William E. Frazier, Nicole Overman, Benjamin Schuessler, Sridhar Niverty *, Timothy Roosendaal, Scott Whalen and Vineet V. Joshi *

Energy and Environment Directorate, Pacific Northwest National Laboratory, Richland, WA 99354, USA; william.frazier@pnnl.gov (W.E.F.); nicole.overman@pnnl.gov (N.O.); benjamin.schuessler@pnnl.gov (B.S.); timothy.roosendaal@pnnl.gov (T.R.); scott.whalen@pnnl.gov (S.W.)

* Correspondence: sridhar.niverty@pnnl.gov (S.N.); vineet.joshi@pnnl.gov (V.V.J.)

Abstract: In the present work, we utilized Shear Assisted Processing and Extrusion (ShAPE), a solid-phase processing technique, to extrude hollow tubes of ZK60 Mg alloy. Hot rolling was performed on these as-extruded tubes (after slitting them longitudinally) to thickness reductions of 37%, 68%, and 93% to investigate their viability as rolling feedstock material. EBSD analysis showed the formation of twinned grains in the ShAPE processed material and a gradual re-orientation of the basal texture parallel to the extrusion direction with each rolling step. Moreover, an equiaxed grain size of 5.15 ± 3.39 μm was obtained in the ShAPE extruded material, and the microstructure was retained even after 93% rolling reduction. The rolled sheets also showed excellent tensile strengths and no mechanical anisotropy, a critical characteristic for formability. The unique microstructures developed and their excellent mechanical properties, combined with the ease of scalability of the process, make ShAPE a promising alternative to existing methods for producing rolling feedstock material.

Keywords: ShAPE; rolling; ZK60; solid phase processing; mechanical anisotropy; texture evolution

check for updates

Citation: Frazier, W.E.; Overman, N.; Schuessler, B.; Niverty, S.; Roosendaal, T.; Whalen, S.; Joshi, V.V. Hot Rolling of ZK60 Magnesium Alloy with Isotropic Tensile Properties from Tubing Made by Shear Assisted Processing and Extrusion (ShAPE). *Appl. Sci.* **2023**, *13*, 5343. https://doi.org/10.3390/app13095343

Academic Editor: Chiara Soffritti

Received: 17 March 2023
Revised: 16 April 2023
Accepted: 19 April 2023
Published: 25 April 2023

Copyright: © 2023 by the authors. Licensee MDPI, Basel, Switzerland. This article is an open access article distributed under the terms and conditions of the Creative Commons Attribution (CC BY) license (https://creativecommons.org/licenses/by/4.0/).

1. Introduction

Magnesium alloys are favorable for the transportation industry owing to their high specific strengths [1]. However, the properties of wrought Mg alloys, like poor formability and mechanical anisotropy, lead to their limited use for lightweight applications [2–4]. The weight percentage of magnesium used in a typical passenger car has remained approximately 0.5% for two decades due to these factors [5,6]. Since the widespread deployment of Mg alloys in the automotive industry could lead to significant improvements in vehicle fuel efficiency, Mg alloy formability has been the subject of considerable research interest.

Mg alloys have low formability at room temperature [3,7,8], although recent experimental work has shown that it is possible to process pure Mg with high formability at room temperature [9]. The reason for this typically low formability was that Mg alloys have a hexagonal close packed (HCP) crystal structure and greatly prefer basal slip when deformed at room temperature [10–13]. However, in order to accommodate plastic deformation, five different slip systems (in addition to twinning) must be active to meet the von Mises criterion [14]. This was a considerable technical obstacle, as prismatic <a>, pyramidal <a>, and pyramidal <a + c> slip all have critical resolved shear stresses that are multiple times higher than basal <a> slip [13]. Numerous strategies exist to circumvent or alleviate this limitation. For example, the addition of Rare Earth (RE) elements to Mg alloys minimizes the critical resolved shear stress (CRSS) to enable additional modes of deformation [15–17]. Other studies have also shown that refining the grain structure promoted grain boundary sliding and improved formability [17–19]. Forming at temperatures between 280 °C and 500 °C generally improves the alloy's deformation response [11,20], but is an energy intensive

process. Twin-roll casting, for example, was a common method used to fabricate Mg alloy sheets [21]. Other authors have attempted to form Mg alloys using multiple cold rolling and annealing steps, such as Zhang et al., who recently achieved refining grain structure and formability in AZ31 through repeated 10–15% cold rolling passes with 30 min intermediate anneals at 250 °C [16]. The anisotropy generated in Mg and Mg alloy from processing are a result of strong basal textures and grain aspect ratios, typically seen after conventional rolling steps. The basal texture introduces a significant anisotropic effect when it comes to tensile deformation properties. The effect of different tensile loading directions on a rolled Mg plate have been studied in the past, emphasizing the anisotropic effect that strong basal texture has on the yield strength, strain hardening behavior and Extension to Failure (ETF) [22–24]. Ideally, elimination of textures and large grain aspect ratios are desired for formability of Mg alloys, and methods for grain refinement are still being studied today.

In order to circumvent the challenges associated with rolling and twin roll casting, several studies have utilized extrusion techniques that cause severe plastic deformation (SPD) to refine the Mg grain structure [17,19]. One of these techniques, equal channel angular processing (ECAP), was also capable of rotating the Mg texture away from the basal texture after multiple passes [12,22]. This process has been able to improve the yield strength, formability, and ETF of Mg alloys [12,22–24] and even their hydrogen storage properties [25]. Unfortunately, the batch size and scalability of this and most other SPD methods are currently limited to amounts that would not be feasible for industrial-level production [5]. However, a new form of Friction Stir Back Extrusion (FSBE) called Shear Assisted Processing and Extrusion (ShAPE) has recently shown promise as a method to control Mg alloy grain size and texture [5,26–29]. ShAPE is a single step solid phase processing technique that allows us to extrude powder, plate chips, and ingots into homogenous and defect-free wrought products. It has several primary advantages over other existing SPD methods. First, unlike ECAP and other methods, ShAPE was able to produce long hollow-section extrusions, which were necessary for application in certain structural components [5]. Second, ShAPE can produce extrusions with large outer diameters and high extrusion ratios in comparison to other FSBE methods, giving it promise as a scalable method. Finally, ShAPE was able to produce extrusions with wall thicknesses of less than a millimeter [26], which means that it could potentially be fabricated and then formed into a sheet with minimal rolling. More recently, the authors have also demonstrated that the properties of ShAPE extruded Mg rods and tubes had isotropic properties with high elongation and better corrosion resistance [30]. Several alloys have so far been extruded using this novel process and this process was agnostic to feedstock material.

ZK60 is the Mg alloy of interest in this study. ZK60 has a moderate cost and favorable ratio of compressive to tensile strength (compared to RE Mg alloys) [31]. SPD techniques such as Equal Channel Angular Pressing (ECAP), Accumulative Roll Bonding (ARB) and Cyclic Extrusion and Compression (CEC) have been employed on ZK60 and other Mg alloys to refine grain size (to the range of 0.6–6 μm) and increase strength while also maintaining favorable ductility [32–39]. Previous work by the current authors employed ShAPE to form ZK60 tubes with average grain size less than 5 μm and to obtain a texture with basal planes oriented 20–45° to the extrusion axis. Interestingly, the ShAPE process also required less than 20 times the force required to form a tube of ZK60 compared to conventional extrusion process, thus providing significant energy savings [29]. The combination of excellent microstructure and properties, combined with the scalability and accompanying energy savings makes post-ShAPE ZK60 an excellent feedstock material for rolling. Thus, the effect of combining ShAPE processing and rolling on the microstructure and mechanical properties of ZK60 is worth exploring.

In the present investigation, we utilized ShAPE processing to form sheets of ZK60 and alleviate some of the challenges associated with the formed product and conventional processes. We hypothesized that the ShAPE extruded ZK60 would retain its microstructure and mechanical properties when formed from a tube into a plate and when subsequently

rolled. Here, we demonstrate the viability of ShAPE extruded ZK60 as rolling feedstock and inform ShAPE processing parameters.

2. Experimental Methods

Extruded ZK60 tubes were fabricated from ZK60-T5 bar and as-cast billets using the method described by Whalen et al. [5]. This resulted in tubes having an outer diameter of 50.8 mm and a wall thickness of 1.9 mm which were sectioned transversely into approximately 200 mm long sections. After this transverse sectioning, the tubes were slit along the extrusion direction and forced open at room temperature using a vice. Figure 1a shows a schematic of the ShAPE process configured to extrude round tubes using a rotating die with a stationary mandrel. Figure 1b shows examples of the as-extruded tubes. Figure 1c shows a schematic of the slitting, opening, and rolling operation, and Figure 1d–f shows the actual sample after slitting, rolling, and cutting into tensile specimens.

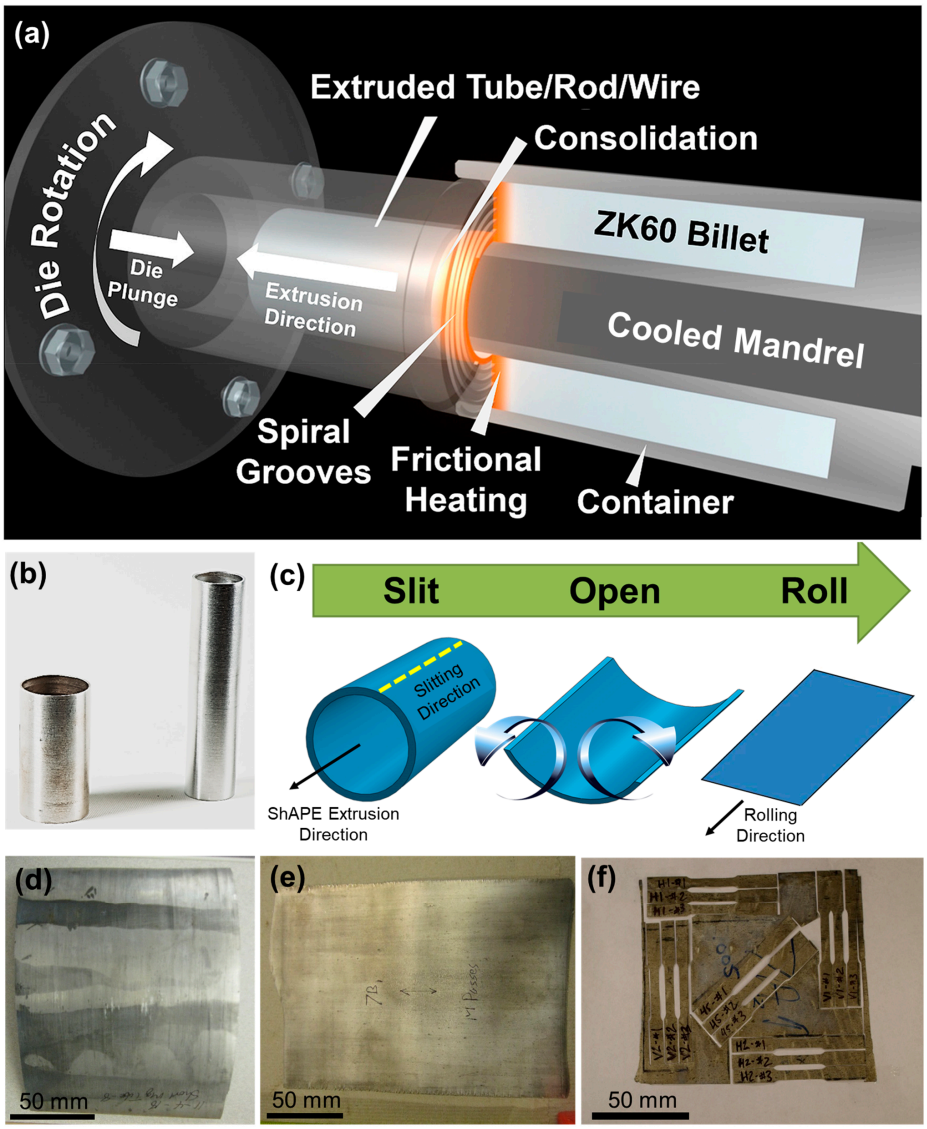


Figure 1. (**a**) A schematic showing the ShAPE process configured to extrude round tubing using a rotating die, (**b**) ShAPE-processed ZK60 tubes before being slit open for rolling. (**c**) A schematic diagram showing the slit, open and roll steps employed to fabricate a rolled sheet from an extruded ZK60 tube. (**d**) Optical photograph of ZK60 tube after slitting along the extrusion axis. (**e**) Rolling of the tube into a flat sheet. (**f**) Tensile specimen cutout of rolled ZK60 sheet.

The flattened plates were then heated in air at 450 °C for periods of five minutes in an air furnace, and then immediately rolled. In order to minimize heat loss, the plates were moved from the furnace to the rollers on a hot plate. For the current work, rolling was performed on a Stanat model TA-215, two-high mill. The top and bottom rolls were 101.6 mm (4 inches) in diameter and approximately 203.2 mm (8 inches) wide. The rolling experiments were performed without any lubrication. The mill was operated at 25 rpm and had a maximum load separation force (LSF) of 445 kN (100,000 lb). Each rolling pass had a targeted reduction of approximately 15%. The 1.9 mm tubes were flattened and rolled until a final thickness of 1.3 mm, 0.64 mm, and 0.13 mm correspond to total reductions of 37%, 68%, and 93%, respectively. Of these, the samples with 37% reduction and 68% reduction were examined using Electron Backscattered Diffraction (EBSD). These levels of reduction were selected because above this level of reduction, patterns became difficult to capture in EBSD. The level of deformation at these reductions introduced a significant amount of strain, enough to decrease the diffraction intensity such that the standard form of Hough indexing was not able to capture the information. For the purpose of comparison, a sample obtained from the flattened tube prior to rolling was also examined using EBSD. Prior to microstructural analysis, specimens were mounted in epoxy and polished to a final surface finish of 0.05 µm using colloidal silica. Scanning electron microscopy (SEM) analysis was performed using a JEOL 7600F field emission scanning electron microscope. EBSD mapping was performed using an Oxford Instruments Nordlys detector at an accelerating voltage of 20 keV and a working distance of ~24 mm. Indexing was accomplished using a magnesium hexagonal crystal structure, Laue group 9, space group 194 and unit cell parameters a = 3.209 Å, b = 3.209 Å, c = 5.211 Å, a = 90°, b = 90°, c = 120°. A step size of 0.1 µm was utilized for these scans. It should be noted that only the matrix phase was mapped for EBSD analysis. Refined second phase precipitates were not included in the EBSD analysis due to the large length scales that the texture evaluation was performed across. From this microscopy, the grain structure of the samples through the thickness was determined using cross sections cut in both the rolling and transverse directions. Pole figures of the grain orientations were also obtained in order to determine any changes in texture.

Mechanical testing of ZK60 specimens was performed using ASTM E8 on a 5K servo-hydraulic load frame using hydraulic knurled wedge grips. The 68% hot-rolled specimens were cut into tensile specimens 29.2 mm long, 6.38 mm wide, and 0.571 mm thick, while the 93% hot-rolled samples were cut into tensile specimens 21.9 mm long, 4.85 mm wide, and 0.157 mm thick as shown in Figure 1c. Optical extensometry (Epsilon ONE-78PT-200 optical extensometer) was used to determine extension with respect to loading. The samples with 68% reduction and 93% reduction were cut into tensile testing specimens oriented in the rolling transverse, and at a 45° angle from the rolling directions, as shown in Figure 1e. This testing allowed us to establish the effect of additional rolling treatment on mechanical performance and anisotropy. Three tensile tests were performed for each specimen thickness and orientation, and from these tests, the 0.02% yield stress, ultimate tensile stress, and % elongation to failure were determined. These results in comparison to the measurements on as-extruded ZK60 from Whalen et al. [5,29] helped us to ascertain the extent to which ShAPE processed ZK60 retains texture, grain structure, and mechanical properties after rolling compared with the as-extruded tube.

3. Results and Discussion

3.1. Microstructural Characterization of As-Extruded, 37% Rolled and 68% Rolled Samples

Longitudinal, through-thickness cross-sections of the ZK60 samples for the ShAPE extruded and flattened, 37% hot-rolled, and 68% hot-rolled sheets are shown in Figure 2**.** In the ShAPE extruded and flattened microstructure, it was observed that the grains were equiaxed. Upon extrusion, in the case of the flattened specimens, the inverse pole figure maps of the microstructure show that twinning (blue bands in the red matrix) had occurred during the flattening process (Figure 2 inset). It should be noted that the flattening

procedure was performed at room temperature. However, the microstructure maintains the majority of its texture and uniformity from Whalen et al. [5].

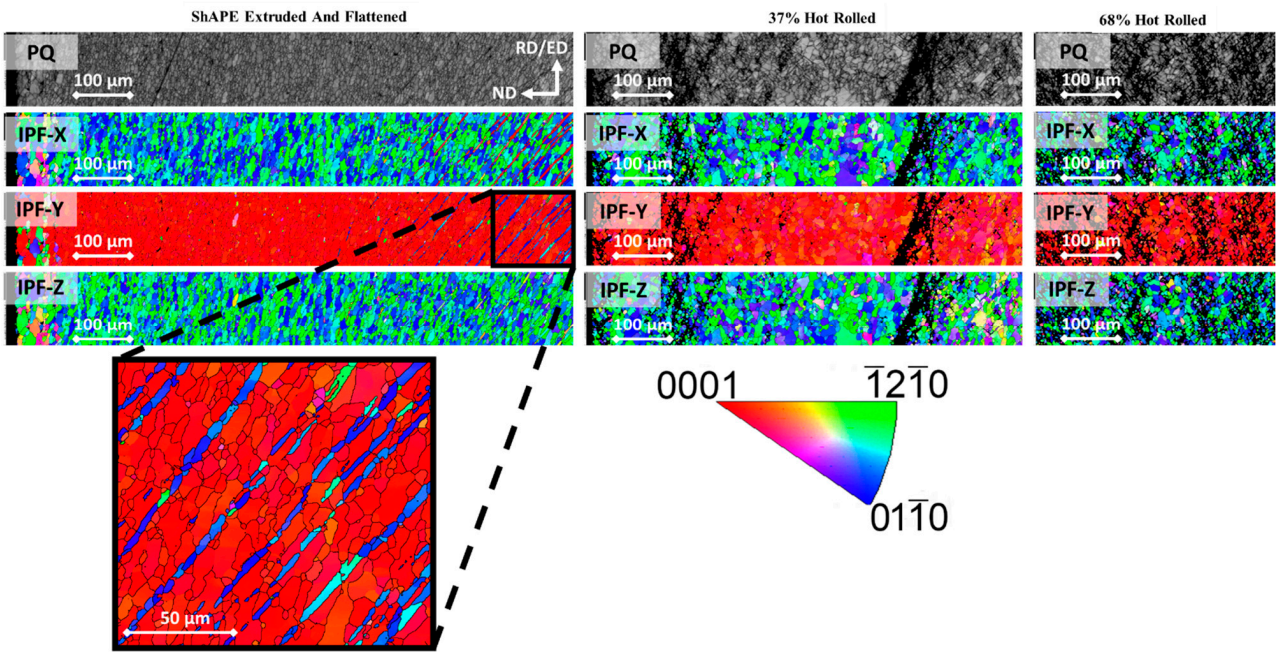


Figure 2. Through-thickness longitudinal EBSD orientation maps of the ShAPE extruded and flattened, 37% hot-rolled, and 68% hot-rolled ZK60 specimens in the longitudinal section. In each map, the left side was the outer diameter of the tube, while the right side was the inner diameter of the tube.

The 37% and 68% rolled plates exhibited the same equiaxed microstructure and were accompanied by bands of low diffraction contrast, resulting in non-indexed pixels. The through-thickness longitudinal EBSD scans of the sheets showed that while the as ShAPE extruded and flattened sheet has a very uniform microstructure, after a 37% reduction there are grains that have visibly grown and deviated from the as-extruded texture. Diffraction bands in Kikuchi patterns from EBSD were notably weaker lending itself unable to determine a grain orientation, which either indicates that the region has been highly deformed or that the region has very fine recrystallized grains. Deformation twinning in Mg alloys has been previously reported by numerous authors [40,41]. The twinned grains were present in the microstructure upon ShAPE processing and flattening the plates. However, they were not seen in the as-ShAPE'd microstructure [5,29]. This shows that they were formed due to the flattening process at room temperature, indicating that these are deformation twins. A measurement of the misorientation profile between the apparent twinned grains confirms that these grains were indeed twinned, as shown in Figure 3.

When plotted to show orientation density, it was observed that the microstructure of the flattened plates showed that the basal planes were approximately tilted 5–10° away from the extrusion direction, as shown in Figure 4. As shown in Figure 4a and its corresponding pole figure in Figure 4d, the tilt of the basal plane is approximately 5–10° away from the extrusion direction. With the applied hot rolling and reheating treatment, the basal planes oriented themselves parallel to the rolling direction. After a 68% reduction, the grain size increased. A similar trend can be seen for transverse sections of the ZK60 samples, as shown in Figure 5. These results also indicate that despite the initial rotation being away from the rolling direction as a result of the ShAPE process, the multiple rolling passes cause texture rotation back towards the rolling direction.

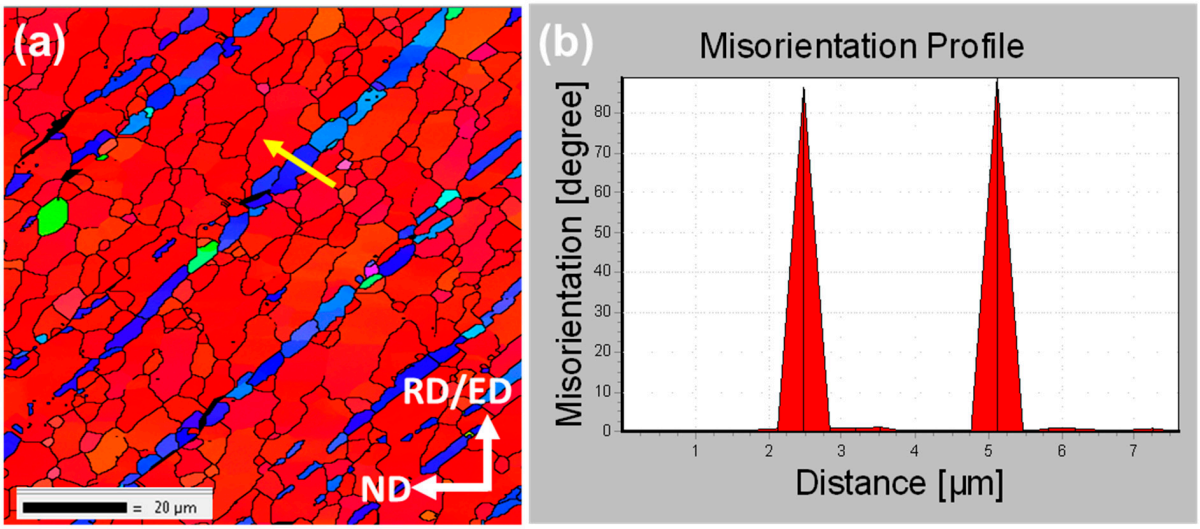


Figure 3. (**a**) Grain orientation (IPF Y) map showing the deformation twinning between two grains in the as-flattened ZK60; (**b**) Misorientation profile on an EBSD map of the as-flattened ZK60 plate. The yellow arrow in Figure 3a indicates the location and direction of the misorientation line profile.

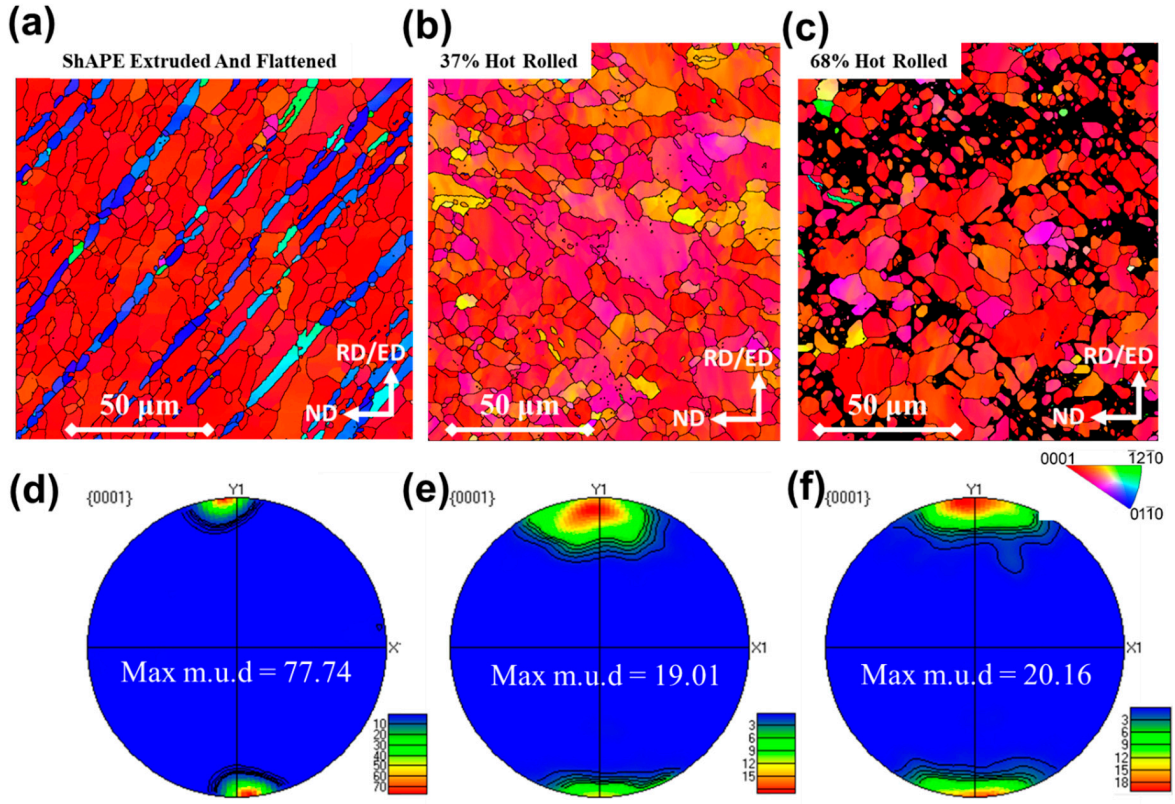


Figure 4. EBSD orientation (IPF Y) maps (**a**–**c**) and their respective pole figures (**d**–**f**) of the ShAPE extruded and flattened, 37% hot-rolled, and 68% hot-rolled ZK60 specimens, respectively, in the longitudinal section.

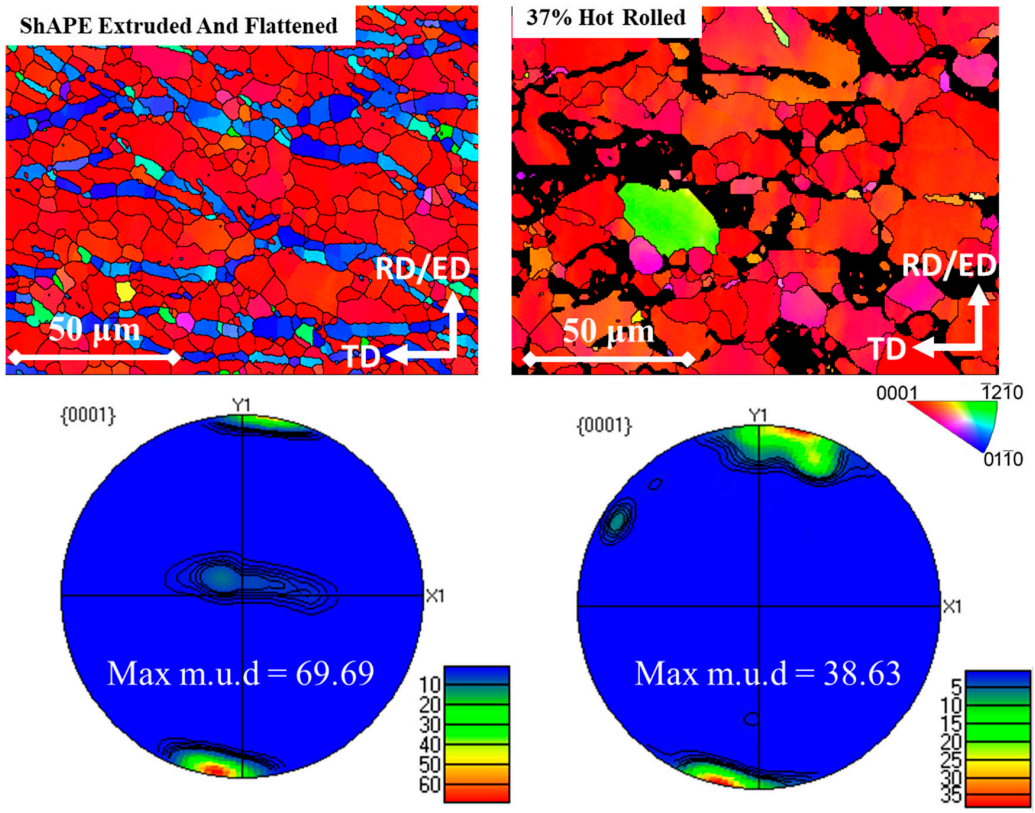


Figure 5. EBSD orientation (IPF Y) maps and pole figures of the ShAPE extruded and flattened and the 37% hot rolled ZK60 specimens in the transverse section.

Plots of the grain size distribution for each rolling condition taken from longitudinal sections indicated relatively small changes in average grain diameter, as shown in Figure 6. Although the rolling process has visibly changed the grain structure, the average grain size remains approximately the same, beginning at 5.15 ± 3.39 µm in the ShAPE extruded material, to 5.27 ± 3.53 µm after 68% rolling reduction. Notably, this excludes the regions of the rolled specimens where obtaining a diffraction pattern was not possible. It was also noticed that while the average grain diameters are the same with respect to rolling extent, the maximum grain size, X_{max}, after hot rolling had increased. From Figure 6, the maximum grain sizes grew from ~19 µm to 33.6 and 26.8 µm after 37% and 68% hot-rolling, respectively.

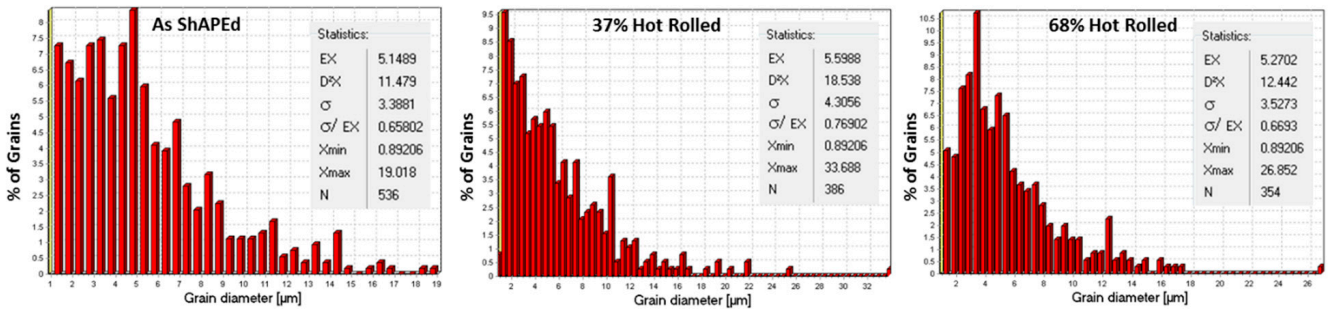


Figure 6. The grain size distributions of ShAPE extruded, 37% hot-rolled, and 68% hot-rolled ZK60 specimens, as taken from EBSD scans on longitudinal sections.

3.2. Mechanical Performance of the Rolled Plates

The tensile properties of the rolled specimen indicate that rolling initially creates an increase in strength at the expense of elongation to, failure. Plots of tensile behavior for 68% rolled specimens in the rolling direction, transverse direction, and 45° to rolling show that ultimate tensile stress (UTS) reaches over 330 MPa in each case, as shown in Figure 7a. This was a significant increase from the measured UTS by Whalen et al. where UTS values of 254.4 MPa, 297.2 MPa and 279.9 MPa were reported for the Longitudinal, Transverse and 45° to longitudinal directions, respectively [29]. However, most of the specimens do not reach 10% extension to failure, which was a significant decrease from Whalen's observations. This behavior was not surprising, as other experimental efforts to form magnesium alloys have also reported increased strength and reduced elongation to failure, even after the use of extrusion processes to refine grain structure and improve texture [12]. It was notable that Whalen et al. reported noticeable anisotropy between the UTS of the rolling, transverse, and 45° tensile specimens, over 40 MPa, while the specimens used in this study have less than 10 MPa of variation. This suggests that hot rolling at this point has reduced the tensile anisotropy of the material.

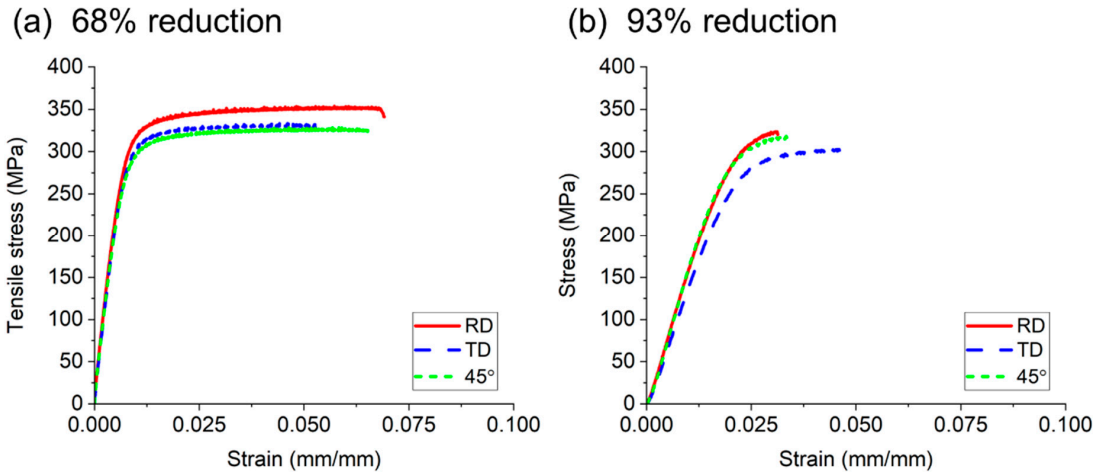


Figure 7. (**a**) Representative tensile stress-strain curves of the ShAPE-processed ZK60 flattened and hot-rolled to 68% reduction. (**b**) Representative tensile stress-strain curves of the ShAPE-processed ZK60 flattened and hot-rolled to 93% reduction. Plots are shown for loading in the rolling direction (RD), 45° to the rolling direction (45°), and the transverse direction (TD).

Additional rolling appears to lead to an overall reduction in tensile properties and an increase in the apparent anisotropy. The 93% rolled specimens, regardless of direction, all have a slightly lower average UTS and smaller elongation to failure (ETF) than the 68% rolled specimens. Considerably more variation in the mechanical behavior was noticeable. The variation in UTS with tensile direction at the same time increased to nearly 25 MPa. This was still less variation than that observed for the ShAPE extruded material. The plots of these tensile stress-strain curves are shown in Figure 7b. The average yield stress, UTS, and ETF for the 68% and 93% rolled specimens was shown in Table 1. Typically, in ZK60, it has been observed that the yield strength along the rolling direction is approximately 50% lesser than in transverse direction. The strength of the plates at both 68% and 93% reduction showed higher values of strength in both transverse and longitudinal directions with no anisotropy as compared to what has been reported in the literature [42].

Table 1. The tensile properties of ShAPE-processed ZK60 after hot rolling.

Direction	68% Reduction			93% Reduction		
	YS (MPa)	UTS (MPa)	ETF %	YS (MPa)	UTS (MPa)	ETF %
RD	292.16 ± 1.11	341.74 ± 5.96	6.95 ± 1.94	256.93 ± 18.4	260.76 ± 22.4	3.38 ± 0.51
TD	286.19 ± 1.13	336.09 ± 1.58	5.15 ± 0.05	251.91 ± 18.9	262.83 ± 21.2	4.00 ± 0.87
45°	284.33 ± 3.18	334.61 ± 2.12	6.31 ± 0.71	272.81 ± 19.1	289.28 ± 14.8	3.64 ± 0.12

It is important to mention, for example, that while the ZK60 sheets in this work were rolled immediately after heating, the sheets were not held at an elevated temperature for rolling, and the rollers themselves were not heated. A hot plate was used to mitigate heat loss in the Mg sheet during transfer to the rolling mill, but it is conceivable that this cooling causes the sheet to experience significant cold work, especially as the sheet decreases in thickness and cools more rapidly. The rolling temperature, annealing treatment, and reduction per pass may also foreseeably improve sheet performance. Previous experimentation on hot-pressed ZK60 by Wang et al. has shown that at annealing temperatures of 400 °C, recrystallization occurred in under 1000 s, and in the same time the grain structure coarsened from roughly 2 μm to 7 μm [10]. This suggests that the time taken to reheat in this work, five minutes (300 s) at 450 °C, should have been sufficient to cause significant static recrystallization, but may not have been enough to entirely recrystallize the material. The work by Wang, amongst others [11,18,43,44], has reported the formation of highly strained bands within the deformed grain structure after rolling, which was similar to our observation in this work for 37% and 68% rolled specimens. It was notable that Wang et al. reports that at 1000 s at 400 °C, the grain structure was completely recrystallized, but that 5000 s of annealing at temperature were required to cause the microstructure to become equiaxed [10]. If the performance of the sheet were affected by this change in the grain structure, then additional annealing may significantly improve its tensile properties.

Examination of the fractured specimens shows that the fracture occurred at an approximately 45° angle with respect to the loading axis in all specimens, regardless of the orientation of the sample or its rolled thickness (e.g., Figure 8). Further improvements in the elongation can be obtained by utilizing a suitable heat treatment process. For example, Jin et al., were able to greatly improve the elongation to failure of ZK60 hot-rolled to a 63% reduction in thickness by using an electropulsing treatment [45]. Understanding the microstructural changes through the flattening of hollow tubes generated via ShAPE was crucial to understand the application limitations and benefits to Mg alloys. The ShAPE-fabricated tubes must retain their properties through flattening and additional forming steps for feasible use as rolling feedstock. This work has demonstrated that the ShAPE extruded tubes can feasibly survive the process of forming into plates. This work has also established that it was possible to hot roll ShAPE extruded ZK60 to the thicknesses required for industrial applications. Modifications to the rolling schedule used in this work has the potential to lead to further improvements over the measured properties.

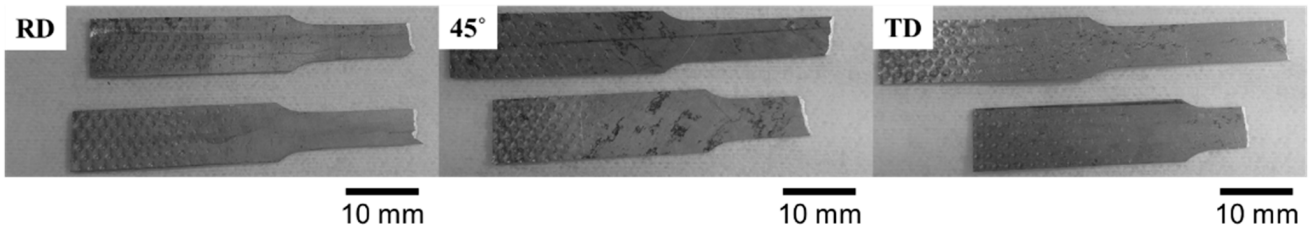


Figure 8. 68% rolled fractured specimens taken from RD, TD and 45° to extrusion axis.

4. Conclusions

ShAPE-processed ZK60 tubes were mechanically slit opened and hot-rolled into thin sheets in order to evaluate the viability of the material as rolling feedstock. The thermomechanical processing pathway indicated that after the ShAPE extrusion, the ZK60 microstructures were resilient to large changes regarding grain sizes and texture. Flattening of ShAPE processed tubes retained the initial ShAPE microstructure. The samples from both the 68% and 93% rolling conditions showed no anisotropy. The development of feedstock material that can largely retain their original microstructure and performance after subsequent deformation processes such as rolling, is both novel and critical. Through this article, we demonstrated that ShAPE processing offers an excellent pathway to produce such feedstock material using Mg alloys.

Author Contributions: W.E.F.: conception, experimental design, carrying out measurements and manuscript composition; N.O.: experimental design and carrying out measurements; B.S.: carrying out measurements and manuscript composition; S.N.: carrying out measurements and manuscript composition; T.R.: experimental design and carrying out measurements; S.W.: conception, experimental design, manuscript composition, and funding acquisition; V.V.J.: conception, experimental design, manuscript composition and funding acquisition. All authors have read and agreed to the published version of the manuscript.

Funding: This work was supported by the Laboratory Directed Research and Development (LDRD)—Technology Investment Program (TIP), 2019, of Pacific Northwest National Laboratory (PNNL). The Pacific Northwest National Laboratory is operated by the Battelle Memorial Institute for the United States Department of Energy under contract DE-AC06-76LO1830.

Institutional Review Board Statement: Not applicable.

Informed Consent Statement: Not applicable.

Data Availability Statement: The data generated during and/or analyzed during the current study is available from the corresponding author on reasonable request.

Acknowledgments: The authors thank Mark Rhodes and Michael Dahl of PNNL for their assistance and advice in the rolling process. The authors thank Rob Seffens, Timothy Roosendaal, and Ethan Nickerson for their assistance in the tensile testing of specimens. The authors also thank Anthony Guzman for his assistance in sample preparation for microstructural characterization. The authors also acknowledge all the other staff directly or indirectly associated with producing the results featured in this publication. This work was supported by the Laboratory Directed Research and Development (LDRD)-Technology Investment Program (TIP), 2019, of Pacific Northwest National Laboratory (PNNL). The Pacific Northwest National Laboratory is operated by the Battelle Memorial Institute for the United States Department of Energy under contract DE-AC06-76LO1830.

Conflicts of Interest: The authors declare no conflict of interest.

References

1. Mordike, B.L.; Ebert, T. Magnesium Properties—Applications—Potential. *Mater. Sci. Eng. A* **2001**, *302*, 37–45. [CrossRef]
2. Aghion, E.; Bronfin, B.; Eliezer, D. The Role of the Magnesium Industry in Protecting the Environment. *J. Mater. Process. Technol.* **2001**, *117*, 381–385. [CrossRef]
3. Hirsch, J.; Al-Samman, T. Superior Light Metals by Texture Engineering: Optimized Aluminum and Magnesium Alloys for Automotive Applications. *Acta Mater.* **2013**, *61*, 818–843. [CrossRef]
4. Joost, W.J.; Krajewski, P.E. Towards Magnesium Alloys for High-Volume Automotive Applications. *Scr. Mater.* **2017**, *128*, 107–112. [CrossRef]
5. Whalen, S.; Overman, N.; Joshi, V.; Varga, T.; Gra, D.; Lavender, C. Magnesium Alloy ZK60 Tubing Made by Shear Assisted Processing and Extrusion (ShAPE). *Mater. Sci. Eng. A* **2019**, *755*, 278–288. [CrossRef]
6. *Lightweight Materials R&D: FY14 Annual Progress Report*; Pacific Northwest National Laboratory: Richland, WA, USA, 2015.
7. Bian, M.Z.; Sasaki, T.T.; Nakata, T.; Kamado, S.; Hono, K. Effects of Rolling Conditions on the Microstructure and Mechanical Properties in a Mg—Al—Ca—Mn—Zn Alloy Sheet. *Mater. Sci. Eng. A* **2018**, *730*, 147–154. [CrossRef]
8. Suh, B.C.; Shim, M.S.; Shin, K.S.; Kim, N.J. Current Issues in Magnesium Sheet Alloys: Where Do We Go from Here? *Scr. Mater.* **2014**, *84–85*, 1–6. [CrossRef]

9. Zeng, Z.; Nie, J.F.; Xu, S.W.; Davies, C.H.J.; Birbilis, N. Super-Formable Pure Magnesium at Room Temperature. *Nat. Commun.* **2017**, *8*, 972. [CrossRef] [PubMed]
10. Wang, S.; Kang, S.B.; Cho, J. Effect of Hot Compression and Annealing on Microstructure Evolution of ZK60 Magnesium Alloys. *J. Mater. Sci.* **2009**, *44*, 5475–5484. [CrossRef]
11. Wang, W.; Chen, W.; Zhang, W.; Cui, G.; Wang, E. *Effect of Deformation Temperature on Texture and Mechanical Properties of ZK60 Magnesium Alloy Sheet Rolled by Multi-Pass Lowered-Temperature Rolling*; Elsevier: Amsterdam, The Netherlands, 2018; Volume 712.
12. Yuan, Y.; Ma, A.; Gou, X.; Jiang, J.; Lu, F.; Song, D.; Zhu, Y. *Superior Mechanical Properties of ZK60 Mg Alloy Processed by Equal Channel Angular Pressing and Rolling*; Elsevier: Amsterdam, The Netherlands, 2015; Volume 630.
13. Styczynski, A.; Hartig, C.; Bohlen, J.; Letzig, D. Cold Rolling Textures in AZ31 Wrought Magnesium Alloy. *Scr. Mater.* **2004**, *50*, 943–947. [CrossRef]
14. Taylor, G.I. Plastic Strain in Metals. *J. Inst. Met.* **1938**, *62*, 307–324.
15. Jahedi, M.; McWilliams, B.A.; Knezevic, M. Deformation and Fracture Mechanisms in WE43 Magnesium-Rare Earth Alloy Fabricated by Direct-Chill Casting and Rolling. *Mater. Sci. Eng. A* **2018**, *726*, 194–207. [CrossRef]
16. Zhang, H.; Cheng, W.; Fan, J.; Xu, B.; Dong, H. Improved Mechanical Properties of AZ31 Magnesium Alloy Sheets by Repeated Cold Rolling and Annealing Using a Small Pass Reduction. *Mater. Sci. Eng. A* **2015**, *637*, 243–250. [CrossRef]
17. Somekawa, H.; Singh, A.; Mukai, T.; Inoue, T. Effect of Alloying Elements on Room Temperature Tensile Ductility in Magnesium Alloys. *Philos. Mag.* **2016**, *96*, 2671–2685. [CrossRef]
18. Guo, H.; Zeng, X.; Fan, J.; Zhang, H.; Zhang, Q.; Li, W.; Dong, H.; Xu, B. Effect of Electropulsing Treatment on Static Recrystallization Behavior of Cold-Rolled Magnesium Alloy ZK60 with Different Reductions. *J. Mater. Sci. Technol.* **2019**, *35*, 1113–1120. [CrossRef]
19. Wei, Y.H.; Wang, Q.D.; Zhu, Y.P.; Zhou, H.T.; Ding, W.J.; Chino, Y.; Mabuchi, M. Superplasticity and Grain Boundary Sliding in Rolled AZ91 Magnesium Alloy at High Strain Rates. *Mater. Sci. Eng. A* **2003**, *360*, 107–115. [CrossRef]
20. Nugmanov, D.; Knezevic, M.; Zecevic, M.; Sitdikov, O.; Markushev, M.; Beyerlein, I.J. Origin of Plastic Anisotropy in (Ultra)-Fine-Grained Mg–Zn–Zr Alloy Processed by Isothermal Multi-Step Forging and Rolling: Experiments and Modeling. *Mater. Sci. Eng. A* **2018**, *713*, 81–93. [CrossRef]
21. Cho, J.H.; Jeong, S.S.; Kang, S.B. Deep Drawing of ZK60 Magnesium Sheets Fabricated Using Ingot and Twin-Roll Casting Methods. *Mater. Des.* **2016**, *110*, 214–224. [CrossRef]
22. Wang, C.; Ma, A.; Sun, J.; Liu, H.; Huang, H.; Yang, Z. Effect of ECAP Process on As-Cast and as-Homogenized Mg-Al-Ca-Mn Alloys with Different Mg2Ca Morphologies. *J. Alloys Compd.* **2019**, *793*, 259–270. [CrossRef]
23. Agnew, S.R.; Horton, J.A.; Lillo, T.M.; Brown, D.W. Enhanced Ductility in Strongly Textured Magnesium Produced by Equal Channel Angular Processing. *Scr. Mater.* **2004**, *50*, 377–381. [CrossRef]
24. Suh, J.; Victoria-Hernandez, J.; Letzig, D.; Golle, R.; Yi, S.; Bohlen, J.; Volk, W. Improvement in Cold Formability of AZ31 Magnesium Alloy Sheets Processed by Equal Channel Angular Pressing. *J. Mater. Process. Technol.* **2014**, *217*, 286–293. [CrossRef]
25. Krystian, M.; Zehetbauer, M.J.; Kropik, H.; Mingler, B.; Krexner, G. Hydrogen Storage Properties of Bulk Nanostructured ZK60 Mg Alloy Processed by Equal Channel Angular Pressing. *J. Alloys. Compd* **2011**, *509*, S449–S455. [CrossRef]
26. Kruska, K.; Clark, T.; Darsell, J.; Overman, N.R.; Whalen, S.A.; Bowden, M.E.; Olszta, M.J.; Kruska, K.; Clark, T.; Stevens, E.L.; et al. Homogenization and Texture Development in Rapidly Solidified AZ91E Consolidated by Shear Assisted Processing and Extrusion (ShAPE). *Mater. Sci. Eng. A* **2017**, *701*, 56–68. [CrossRef]
27. Darsell, J.T.; Overman, N.R.; Joshi, V.V.; Whalen, S.A.; Mathaudhu, S.N. Shear Assisted Processing and Extrusion (ShAPE Ô) of AZ91E Flake: A Study of Tooling Features and Processing Effects. *J. Mater. Eng. Perform.* **2018**, *27*, 4150–4161. [CrossRef]
28. Jamalian, M.; Joshi, V.V.; Whalen, S.; Lavender, C.; Field, D.P. Microstructure and Texture Evolution of Magnesium Alloy after Shear Assisted Processing and Extrusion (ShAPE TM). In Proceedings of the IOP Conference Series: Materials Science and Engineering, St George, UT, USA, 6–10 November 2017; Volume 375, p. 012007. [CrossRef]
29. Whalen, S.; Joshi, V.; Overman, N.; Caldwell, D.; Lavender, C.; Skszek, T. Scaled-Up Fabrication of Thin-Walled ZK60 Tubing Using Shear Assisted Processing and Extrusion (ShAPE). In *Magnesium Technology*; Springer: Berlin/Heidelberg, Germany, 2017; ISBN 9783319523927.
30. Beura, V.; Zhang, D.; Overman, N.; Darsell, J.; Herling, D.R.; Solanki, K.; Joshi, V.V. Enhanced Mechanical Behavior and Corrosion Resistance of AZ31 Magnesium Alloy through a Novel Solid-Phase Processing. *Corros. Sci.* **2022**, *197*. [CrossRef]
31. Choi, J.P.; Lavender, C.; Mattlin, K.; Dahl, M. *High-Temperature Aluminum Alloys*; Pacific Northwest National Laboratory: Richland, WA, USA, DOE Annual Merit Review; 2013.
32. Dumitru, F.D.; Higuera-Cobos, O.F.; Cabrera, J.M. ZK60 Alloy Processed by ECAP: Microstructural, Physical and Mechanical Characterization. *Mater. Sci. Eng. A* **2014**, *594*, 32–39. [CrossRef]
33. Lin, J.; Wang, Q.; Peng, L.; Roven, H.J. Microstructure and High Tensile Ductility of ZK60 Magnesium Alloy Processed by Cyclic Extrusion and Compression. *J. Alloys Compd.* **2009**, *476*, 441–445. [CrossRef]
34. Xu, C.; Zheng, M.Y.; Chang, H.; Hu, X.S.; Wu, K.; Gan, W.M.; Brokmeier, H.G. Microstructure and Properties of Pure Mg/ZK60 Laminate Processed by Accumulative Roll Bonding. *Mater. Sci. Forum* **2010**, *650*, 343–346. [CrossRef]
35. Huang, W.; Huo, Q.; Fang, Z.; Xiao, Z.; Yin, Y.; Tan, Z.; Yang, X. Damage Analysis of Hot-Rolled AZ31 Mg Alloy Sheet during Uniaxial Tensile Testing under Different Loading Directions. *Mater. Sci. Eng. A* **2018**, *710*, 289–299. [CrossRef]

36. Wei, Y.; Lu, L.; Li, M.; Ma, M.; Huang, W.; Zhao, X.; Wu, R. Effect of 90° Route on Microstructure of AZ31 Magnesium Alloy Sheets by Forging-Bending Repeated Deformation. *J. Alloys Compd.* **2023**, *948*, 169720. [CrossRef]
37. Yi, S.B.; Davies, C.H.J.; Brokmeier, H.G.; Bolmaro, R.E.; Kainer, K.U.; Homeyer, J. Deformation and Texture Evolution in AZ31 Magnesium Alloy during Uniaxial Loading. *Acta Mater.* **2006**, *54*, 549–562. [CrossRef]
38. Liu, X.; Wang, Y.; Zhu, B.; Xie, C.; Sun, Y.; Yang, H. Effect of Microstructures and Textures on the Anisotropy of Mechanical Properties of AZ31 Magnesium Alloy Sheets Subjected to High Strain Rate Rolling. *Mater. Res. Express* **2019**, *6*, 106591. [CrossRef]
39. Su, H.; Chu, Z.; Xue, C.; Li, Y.; Ma, L. Relationship among Initial Texture, Deformation Mechanism, Mechanical Properties, and Texture Evolution during Uniaxial Compression of Az31 Magnesium Alloy. *Crystals* **2020**, *10*, 1–12. [CrossRef]
40. Beyerlein, I.J.; McCabe, R.J.; Tomé, C.N. Effect of Microstructure on the Nucleation of Deformation Twins in Polycrystalline High-Purity Magnesium: A Multi-Scale Modeling Study. *J. Mech. Phys. Solids* **2011**, *59*, 988–1003. [CrossRef]
41. Wu, X.L.; Youssef, K.M.; Koch, C.C.; Mathaudhu, S.N.; Kecskés, L.J.; Zhu, Y.T. Deformation Twinning in a Nanocrystalline Hcp Mg Alloy. *Scr. Mater.* **2011**, *64*, 213–216. [CrossRef]
42. Fereshteh-Saniee, F.; Fakhar, N.; Karami, F.; Mahmudi, R. Superior Ductility and Strength Enhancement of ZK60 Magnesium Sheets Processed by a Combination of Repeated Upsetting and Forward Extrusion. *Mater. Sci. Eng. A* **2016**, *673*, 450–457. [CrossRef]
43. Yi, D.; Gu, W.; Fang, X.; Wang, B.; Luo, W. Plastic Deformation Behaviors and Dynamic Recrystallization Mechanisms of ZK60 Magnesium Alloy. *Int. J. Soc. Mater. Eng. Resour.* **2006**, *14*, 33–39. [CrossRef]
44. Gong, X.; Gong, W.; Bong, S.; Hyung, J. Effect of Warm Rolling on Microstructure and Mechanical Properties of Twin-Roll Casted ZK60 Alloy Sheets. *Mater. Res.* **2015**, *18*, 360–364. [CrossRef]
45. Jin, W.; Fan, J.; Zhang, H.; Liu, Y.; Dong, H.; Xu, B. Microstructure, Mechanical Properties and Static Recrystallization Behavior of the Rolled ZK60 Magnesium Alloy Sheets Processed by Electropulsing Treatment. *J. Alloys Compd.* **2015**, *646*, 1–9. [CrossRef]

Disclaimer/Publisher's Note: The statements, opinions and data contained in all publications are solely those of the individual author(s) and contributor(s) and not of MDPI and/or the editor(s). MDPI and/or the editor(s) disclaim responsibility for any injury to people or property resulting from any ideas, methods, instructions or products referred to in the content.